

# Energy flow calibration of LHCb ECAL

K. Voronchev<sup>1</sup>

*Institute for Theoretical and Experimental Physics, Moscow, Russia*

I. Belyaev<sup>2</sup>

*Syracuse University, USA*

## Abstract

ECAL is a part of the LHCb calorimeter system consisting of more than 6000 individual readout cells. A good ECAL calibration is essential for overall detector performance. In this article one possible calibration method is described in details.

---

<sup>1</sup>kirill.voronchev@cern.ch

<sup>2</sup>ibelyaev@physics.syr.edu

# 1 Introduction

The electromagnetic calorimeter, ECAL, is part of the calorimeter system [1] of the LHCb detector [2] - a forward single-arm spectrometer for B-physics. The calorimeter system also comprises the scintillator pad detector, SPD, the preshower detector, PS, and the hadronic calorimeter, HCAL. The ECAL detector covers a surface of  $50m^2$ . The calorimeter wall is built out of 3300 detector modules, consisting of 6016 individual readout cells. The calorimeter is divided into 3 sections with different granularity- inner, middle and outer.

ECAL has to comply with the following requirements:

- an energy resolution of  $\sigma_E/E$   $10\%/\sqrt{E} \oplus 1\%$  ( $E$  in  $GeV$ )
- the provision of an essential part of L0 high  $E_T$  trigger;
- a reliable  $e/h$  separation over the full momentum range;
- a performance allowing the reconstruction of B-meson decay channels including photons and  $\pi^0$ 's.

A good ECAL calibration is essential to the performance of trigger algorithms, in order to minimize the mass peak width of reconstructed particles and to reduce the background level. In order to keep the resolution of the calorimeter at the required level, the whole readout chain, consisting of calorimeter cells, PMTs and ADCs has to be calibrated. Several different types of calibration methods were considered for the overall calibration [3]. The current note describes the energy flow method, one of the possible methods to be implemented.

From the precalibration with cosmic particles of ECAL modules it is known that their response is equal within a precision of better than 10% [4]. The purpose of the energy flow method (smoothing method) is to improve this calibration to the order of about 5% for the subsequent calibration procedures with particles ( $\pi^0$  and  $e^-$  calibrations). It should be considered as a first step in an overall calibration of the whole ECAL, and should therefore be fast, robust and simple.

## 2 Energy flow method

### 2.1 General idea

It is supposed that transverse energy flow measured by ECAL, accumulated over a large number of events and binned in ECAL cells is a locally smooth

function. However this smooth behaviour can be affected by the following reasons:

- local material nonuniformity in the area upstream of ECAL
- statistical fluctuations in collected data;
- difference in modules response (miscalibration, malfunctioning, breakdowns)

Material nonuniformity distorts the  $E_T$  distribution but its effect can be estimated by Monte Carlo studies. The statistical fluctuations can be suppressed by collecting large data samples. The remaining main reason for non-smooth behaviour of the transverse energy flow distribution is the difference in individual module response caused by their miscalibration. The point of the method is to assign calibration coefficients to each cell and adjust them until the original non-smooth energy flow distribution is transformed into a smooth one. The required calibration coefficient  $\mathbb{C}_{cal}$  for a given channel  $i$  is the ratio of the final transverse energy value after smoothing the 2D histogram,  $E_T^{smooth}$ , to the original value of  $E_T$ :

$$\mathbb{C}_{cal}^i = \frac{E_T^{smooth}(i)}{E_T(i)} \quad (1)$$

## 2.2 Method description

The study reported in this article was made using minimum bias events that passed the L0 trigger (RTTC production) [5]. They are a good approximation of the events that reach the Event Filter Farm [6] in the real experiment. The transverse energy distribution is accumulated in a 2D histogram reflecting the number and position of the ECAL cells. The transverse energy of a cell is included in the sum if it is above 20 MeV in order to suppress threshold and noise effects<sup>3</sup>. The smoothing algorithm is described in Appendix A. At this stage a perfect calibration has been assumed.

We will refer to this 2D histogram as *initial* (see Fig. 3, left).

The method accuracy can be estimated by smoothing this *initial* histogram.

For data from this calibrated calorimeter (MC simulated) the coefficients from Eq. 1 are by definition  $\mathbb{C}_{cal}^{MC} = 1$ . A variable measuring the difference in the coefficients before and after smoothing is defined as:

$$\varkappa = \frac{\mathbb{C}_{cal}^{MC} - \mathbb{C}_{cal}}{\mathbb{C}_{cal}^{MC}} \quad (2)$$

---

<sup>3</sup>The expected noise is at the level of 1-2 MeV so this cut is well above that value.

will give the measure of the precision of the method.

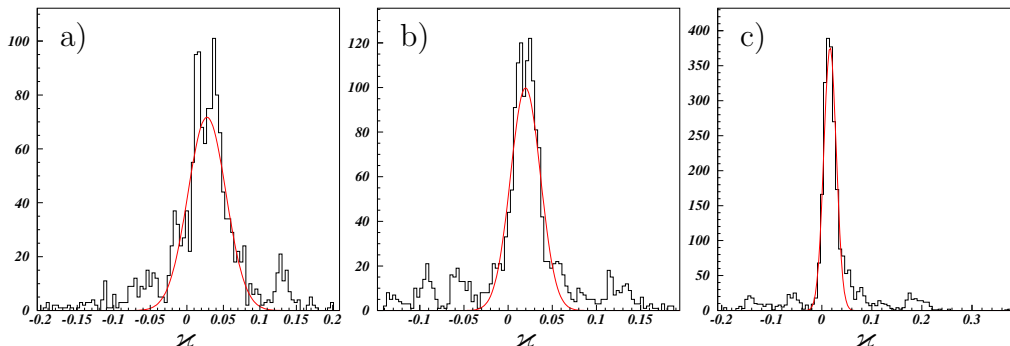


Figure 1: The distributions of  $\varkappa$  for different ECAL zones: a) inner ( $\sigma_{\varkappa}^{init} = 2.6\%$ ), b) middle ( $\sigma_{\varkappa}^{init} = 1.6\%$ ) and c) outer ( $\sigma_{\varkappa}^{init} = 1.2\%$ ) ECAL zones.

The distributions of  $\varkappa$  for all the cells are presented in Figs. 1, 4 for the three calorimeter zones and can each be fit with a Gaussian. The sigmas of these Gaussians, referred to throughout this article as a  $\sigma_{\varkappa}$ , a measure of the overall calibration accuracy, are  $\sigma_{\varkappa}^{init}$ , 2.6% for the inner ECAL zone, 1.6% for the middle zone and 1.2% for the outer zone. Given a sufficient number of events the result of smoothing the *initial* histogram will be affected only by internal limitations of the smoothing procedure.

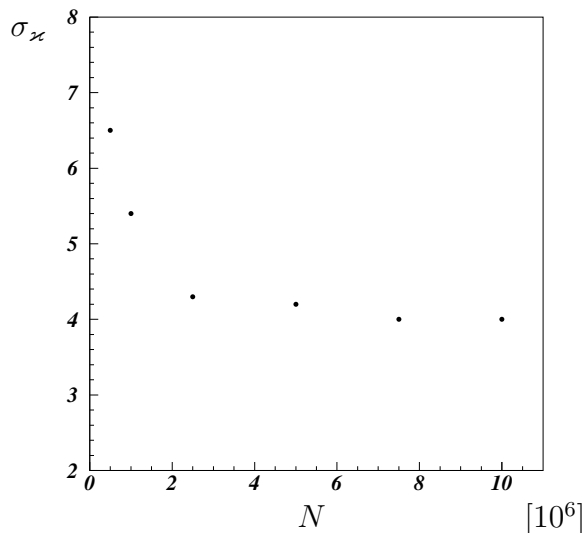


Figure 2: The dependence of  $\sigma_{\varkappa}$  on statistics for inner ECAL zone.

The effect of statistics was studied by measuring  $\sigma_{\varkappa}$  as a function of the number of events treated. In Fig. 2 it is seen that after a few million of processed events a plateau is reached in the accuracy, i.e. after a certain number of events statistical effects (see sec. 2.1) become negligible in comparison with other effects. We conclude that at the level of 10M minimum bias events the accuracy of the method is not influenced by the statistics. At the event rate of 1MHz that can be treated by the event processing farm this event sample can be collected in 10 seconds.

To emulate possible cell miscalibrations arising from module and electronics miscalibrations an artificial cell by cell distortion,  $\mathcal{C}_{dist}$ , distributed according to a Gaussian with a width of 20% was added to the *initial*  $E_T$  distribution, resulting in a *distorted* 2D histogram (see Fig. 3, center). This distorted distribution is then smoothed thus producing a *smoothed* histogram (see Fig. 3, right).

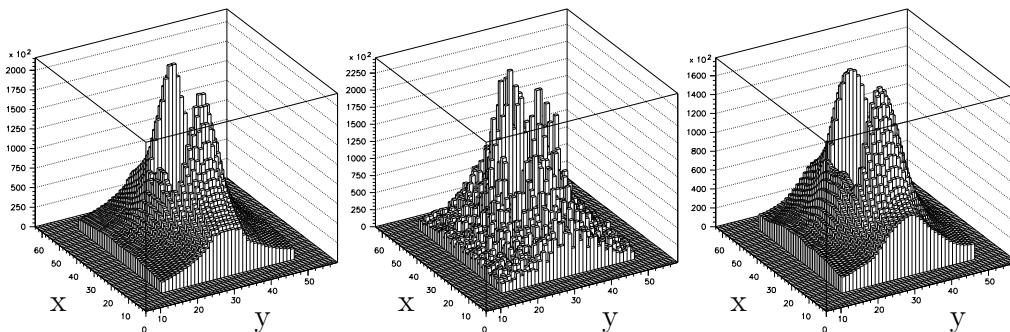


Figure 3: 2D cell by cell histograms of ECAL  $E_T$ : *left*: initial, *center*: distorted, *right*: smoothed, as defined in the text.

## 2.3 Results

The distributions of  $\varkappa$  as defined in Eq. 2 obtained after smoothing the distorted distributions for the case is shown in Fig. 4 for the three ECAL zones.

The results of Gaussian fits to these distributions are given in Tab. 1. With the current smoothing algorithm random 20% miscalibrations can be reduced to about 5%. The fact that the mean values of these distribution are not equal to zero means that the smoothing method introduces some bias to the calibration coefficients. The plots clearly display non-Gaussian tails. These tails mean that some channels are poorly calibrated. To visualize the

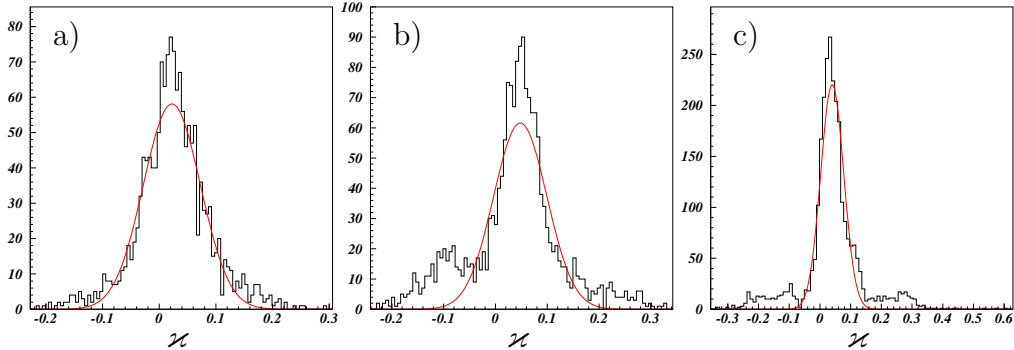


Figure 4: Distributions of  $z$  for different ECAL zones after the smoothing: a) inner, b) middle, c) outer.

Table 1: *Smoothing results for different ECAL zones, in %.*

	$\sigma_z$	RMS	bias
INNER	5	6.4	2.2
MIDDLE	5.1	8.8	4.8
OUTER	3.7	9.5	4

areas with poor calibration efficiency 2D color plots of  $z$  were made. In Fig. 5 negative and positive pulls for the variable  $z$  are shown.

The miscalibration of cells with poorly estimated calibration coefficients can be up to 60%. These cells are not necessarily close to one another and are located predominantly at the zone edges. This is due to the fact that they have fewer neighbors than other cells for the smoothing algorithm to use. On Fig. 4 (middle) the local effects are clearly seen. The middle zone of ECAL has least cells in the horizontal direction, i.e. less neighbors for the smoothing algorithm, thus the  $z$  distribution gets worse. To reduce this bias neighboring cells from adjacent zones must also be included in the smoothing process. This was done for the middle zone by introducing fake cells made of modules from adjacent zones: the calibration becomes more precise (see Fig. 6). Unfortunately nothing can be done with inner cells that surround the beam pipe and outer cells on the edge of ECAL.

The choice of 20% random miscalibrations seems to be slightly above the expected value for the existing precalibration and possible effects caused by electronics. In Fig. 7 the accuracy of the smoothing method ( $\sigma_z^{dist}$ ) is given as a function of original miscalibration values.

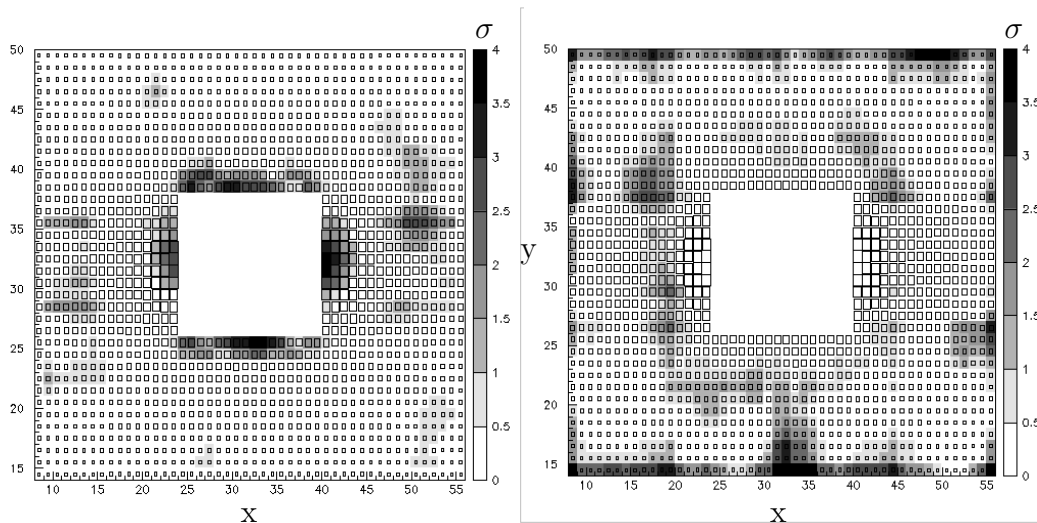


Figure 5: Pull distributions for  $\varkappa$  for inner ECAL zones, *left*: for positive values of deviation, *right*: for negative.

In fact in a real detector there can be not only a random miscalibration but also a systematic one. It can be caused, for instance, by the effect of gain settings of PMTs. The outermost cells of the outer ECAL sections will be working at a gain of  $10^4$ . The performance of PMTs at this gain is well measured. For the cells closer to the beam pipe the gain is lower. The HV settings for lower gains are known with a lower precision leading to incorrect gains and therefore to a systematic miscalibration across the calorimeter face. This kind of distortion can be simulated by introducing a linear miscalibration as a function of distance from the beam pipe,  $d(r)$ . It was chosen to be 30% for the innermost cells ( $r = 30\text{cm}$ ) and 0 at outer cells ( $r = 4\text{m}$ ). For the final studies both a random 20% miscalibration and a linear one were taken into account. The smoothing was performed by the same method.

In Fig. 8 the dependence of the final miscalibration after smoothing for all zones on the distance from the beam pipe is shown along with the initial distortion. It is clearly visible that although the random miscalibration can be suppressed to a good precision of about 5%, the linear part remains. So if in real experiment there will be some sort of systematic miscalibration it will affect the global calibration precision.

These local effects were further investigated. In Fig. 9 the correlation

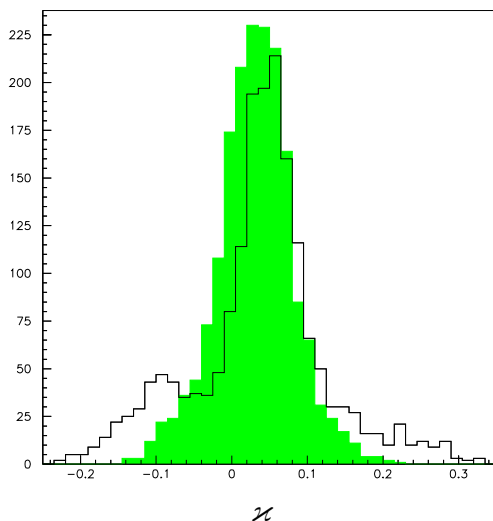


Figure 6: *Shaded*:  $\varkappa$  distribution for the middle zone after the addition of fake cells defined in the text ( $\sigma_{\varkappa}^{dist} = 4.6\%$ ,  $RMS = 5.1\%$ ), *solid*: w/o fake cells ( $\sigma_{\varkappa}^{dist} = 5.1\%$ ,  $RMS = 8.8\%$ ).

function defined as

$$C(r) = \left\langle \frac{(\varkappa_i - \bar{\varkappa}_i)}{\sigma_i} \frac{(\varkappa_j - \bar{\varkappa}_j)}{\sigma_j} \right\rangle \Big|_{|i-j|=r}$$

is shown. The correlation length is defined as

$$\frac{1}{\lambda} = - \left. \frac{d \ln C}{dr} \right|_{r \rightarrow 0}$$

On the plot of the correlation function on Fig. 9 the correlation over the area of about 2 adjacent cells can be seen: in a matrix of 3x3 cells, calibration coefficients are correlated at the level of above 75%.

The possible effect of “dead” channels was also studied. It was found that a few isolated cells with no response do not pose problems to the smoothing algorithm. The final  $\sigma_{\varkappa}^{dist}$  distribution is distorted by about 0.2%.

### 3 Conclusions

This method seems to be a good starting point for the final ECAL calibration. It is simple, robust and fast.

The advantage of this method is that it doesn’t rely on other subdetectors. It can be implemented right after the start of the LHC beam. Even beam gas interactions collected during pilot runs can produce the necessary  $E_T$  distributions.



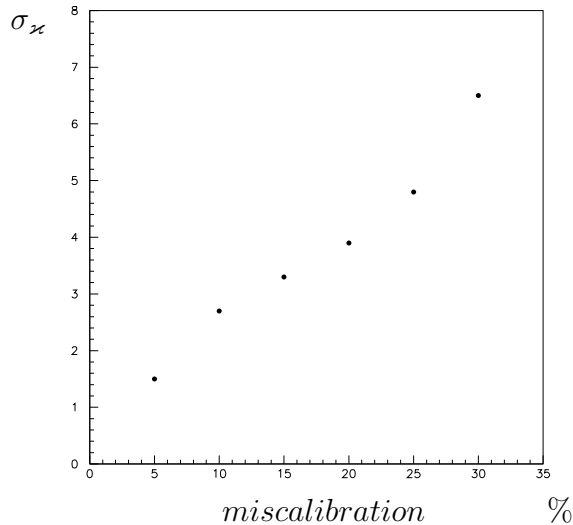


Figure 7: Calibration precision  $\sigma_z^{dist}$  as a function of initial miscalibration for outer ECAL zone.

Although this method doesn't give a good absolute calibration it provides a good relative calibration of ECAL cells. The overall calibration coefficients,  $\mathbb{C}_{cal}$ , may differ significantly from one area of ECAL to another because of systematic miscalibration but locally these coefficients seem to be correlated. This seems important for the subsequent calibration methods (e.g.  $\pi_0$ ).

Once the smooth response from ECAL is established it can be used subsequently to monitor the stability of the detector. The HERA-B collaboration has shown that the transverse energy flow shape remains constant over a long period of time. Any malfunctioning in ECAL modules will immediately distort the smooth behavior of the transverse energy distribution and will become visible in the energy flow distributions in just a few seconds. By comparing a 2D  $E_T$  histogram to one taken a short time earlier it is possible to detect such unwanted changes (e.g. fall of HV). Alternatively if the final calibration is done the energy flow distribution can be used as a standard for the subsequent calibrations during short shutdowns or pause periods thus improving the overall calibration.

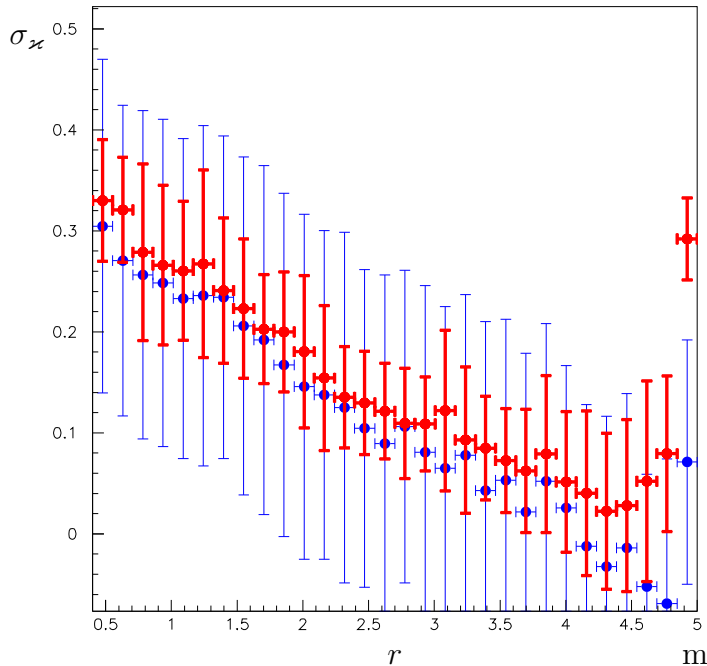


Figure 8: The resulting  $\varkappa(r)$  distribution after smoothing (red) and initial miscalibration (blue).

## A Smoothing algorithm

At first for smoothing 2D histogram of energy flow distributions a standard multiquadric algorithm [7] was implemented. This algorithm turned out to be very parameter sensitive. It depended strongly on parameters of sensitivity to statistical fluctuations and curvatures of the multi-quadric basis function, on the shape of  $E_T$  distribution and also on prescribed bin content uncertainties.

As a simple alternative the following algorithm was introduced:

$$E_{cell} \iff \alpha E_0 + \sum (1 - \alpha) E'_i,$$

where  $E_0$  is the energy of a given cell and  $\sum E'_i$  - the sum of energies of its surrounding cells, i.e. for a given 2D histogram bin representing a single ECAL cell, its value is substituted by a sum of a fraction of its initial energy deposition plus some fraction of its neighbouring bins (cells). This algorithm seems to be robust and simple. It was found that  $\alpha = 0.25$  and that 5 iterations give the best result.

The dependence of  $\sigma_\varkappa$  extracted using the smoothing algorithm described above on the number of iterations is given in Fig. 10.

As is seen from this plot the drawback of this algorithm is that it starts

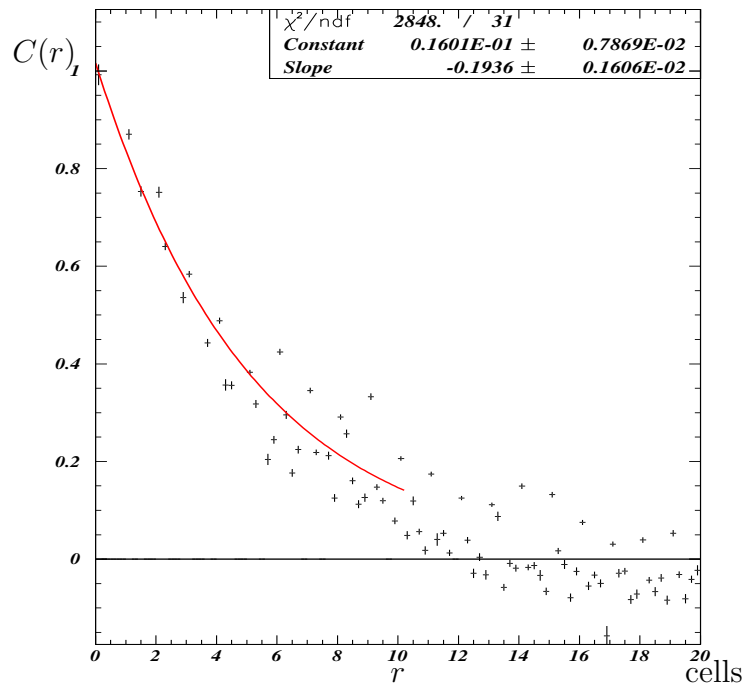


Figure 9: Correlation function for ECAL miscalibration.

to diverge as the number of iterations increases.

In any case smoothing is performed using a certain algorithm not a MC function derived from some studies or any other known parametrization and the result of smoothing does not depend strongly on the smoothing method.

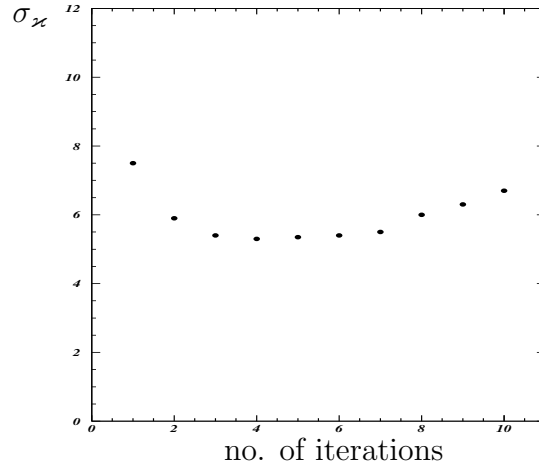


Figure 10: Dependence of smoothing accuracy on number of iterations.

## References

- [1] LHCb Calorimeters, *Technical Design Report*, CERN/LHCC/2000-0036.
- [2] LHCb Reoptimized Detector, Design and Performance, *Technical Design Report*, CERN/LHCC/2003-030.
- [3] On the possibility of in situ calibration of LHCb calorimeters, LHCb-2000-051.
- [4] Design, construction, quality control and cosmic test of ECAL modules for the LHCb experiment, yet to be published
- [5] LHCb Trigger System Technical Design Report, CERN/LHCC/2003-031.
- [6] Neufeld N., Implementation of the LHCb event filter farm, LHCb-2001-143.
- [7] <http://wwwasdoc.web.cern.ch/wwwasdoc/hbook/H2Quadratic-fits.html#HQUAD>